New insight into Cainozoic sedimentary basins and Palaeozoic suture zones in southeast Australia from ambient noise surface wave tomography

P. Arroucau,[1] N. Rawlinson,[1] and M. Sambridge[1]

Received 30 November 2009; revised 27 January 2010; accepted 19 February 2010; published 6 April 2010.

[1] Detailed images of Rayleigh wave group velocity are derived from ambient seismic noise recorded by WOMBAT, a large rolling seismic array project in southeast Australia. Group velocity maps sensitive to crustal structure exhibit low velocity anomalies in the presence of sedimentary basins and recent hot-spot volcanism, and high velocities in regions of out-cropping metamorphic and igneous rocks. Distinct and well-constrained patches of low velocity within the Murray Basin provide new insight into the spatial extent and possible composition of pre-Tertiary infra-basins. In a broader tectonic context, our results show little evidence for the Palaeozoic building blocks of the southeast Australian continent that have been inferred from geological mapping and potential field data. This may mean that apparent changes in basement terrane near the surface are not associated with major changes in composition at depth. **Citation:** Arroucau, P., N. Rawlinson, and M. Sambridge (2010), New insight into Cainozoic sedimentary basins and Palaeozoic suture zones in southeast Australia from ambient noise surface wave tomography, *Geophys. Res. Lett.*, *37*, L07303, doi:10.1029/2009GL041974.

1. Introduction

[2] The Tasmanides of eastern Australia consist of a series of accretionary orogens that formed as a result of convergence along the proto-Pacific margin of east Gondwana [*Glen*, 2005]. Occupying approximately the eastern one third of the Australian continent, the Tasmanides abut the Proterozoic and Archean terranes of western Australia along the so-called Tasman Line, a largely inferred lithospheric scale suture zone, the location and distinctiveness of which remains controversial [*Direen and Crawford*, 2003; *Kennett et al.*, 2004]. In southeast Australia, the Tasmanides comprise the Mid-Late Cambrian Delamerian Fold Belt and the Late Cambrian to Mid-Late Devonian Lachlan Fold Belt (see Figure 1a). The Palaeozoic evolution of these orogens is not well understood due largely to the presence of younger Mesozoic-Cainozoic sedimentary and volcanic cover sequences which mask a significant proportion of the crystalline basement [*VandenBerg*, 1999; *Foster and Gray*, 2000; *Spaggiari et al.*, 2004].

[3] The vast intra-cratonic Murray Basin (see Figure 1a), which obscures large areas of both the Delamerian and Lachlan fold belts, is composed of a thin layer of almost flat-lying and largely marine Tertiary sediments overlain by a complex of fluvial and aeolian Quaternary sediments [*Knight et al.*, 1995]. Results from drilling and interpretation of gravity and magnetic data reveal the presence of a number of pre-Tertiary infra-basins concealed beneath the Murray Basin [*Knight et al.*, 1995]; these formed in the Late Palaeozoic and appear to be aligned with the strike of the basement terrane, suggesting that they are associated with grabens and downwarps of the underlying crust. Other basins in the region include the Otway, Bass and Gippsland basins (Figure 1a), which were initiated by the break-up of Australia and Antarctica during the Cretaceous [*Bryan et al.*, 1997], and the Sydney Basin, a Permian-Triassic foreland basin. Further complicating interpretation of the Palaeozoic terrane is the presence of the Newer Volcanic Provinces (NVP) in western Victoria, an extensive cover of Quaternary basalt that originates from hot-spot volcanism [*Price et al.*, 1997].

[4] In an attempt to better understand the lithospheric structure and tectonic evolution of southeast Australia, an on-going series of passive seismic array deployments have been carried out in the region. To date, over 500 sites have been occupied during 12 consecutive deployments, with station spacing varying between 15 km (in Tasmania) and 50 km (on the mainland). The passive seismic data recorded so far has played a major role in unravelling the structure of the lithosphere in southeast Australia. This has mainly been in the form of teleseismic tomography [*Graeber et al.*, 2002; *Rawlinson et al.*, 2006b, 2006a; *Clifford et al.*, 2008; *Rawlinson and Kennett*, 2008] or combined wide-angle and teleseismic tomography [*Rawlinson and Urvoy*, 2006], the latter of which is restricted to Tasmania.

[5] In this study, ambient noise tomography [e.g., *Shapiro et al.*, 2005; *Villaseñor et al.*, 2007] is applied to WOMBAT data for the first time in order to image the crustal structure beneath southeast Australia. To date, the only other ambient noise tomography study carried out in Australia [*Saygin and Kennett*, 2009] has produced continent-wide maps of Rayleigh wave group velocity using temporary and permanent broadband installations, resulting in a horizontal resolution upwards of 200 km. Due to the much denser spacing of WOMBAT stations, horizontal resolution upwards of 40 km can be expected in mainland southeast Australia, which will result in the elucidation of much finer scale structure compared to the continental scale maps.

2. Data and Method

[6] The focus of this study is ambient noise data from seven of the mainland arrays of the WOMBAT project (Figure 1b) which spans much of the Delamerian and Lachlan orogens. The total number of stations used is 282,

[1]Research School of Earth Sciences, Australian National University, Canberra, ACT, Australia.

0094-8276/10/2009GL041974

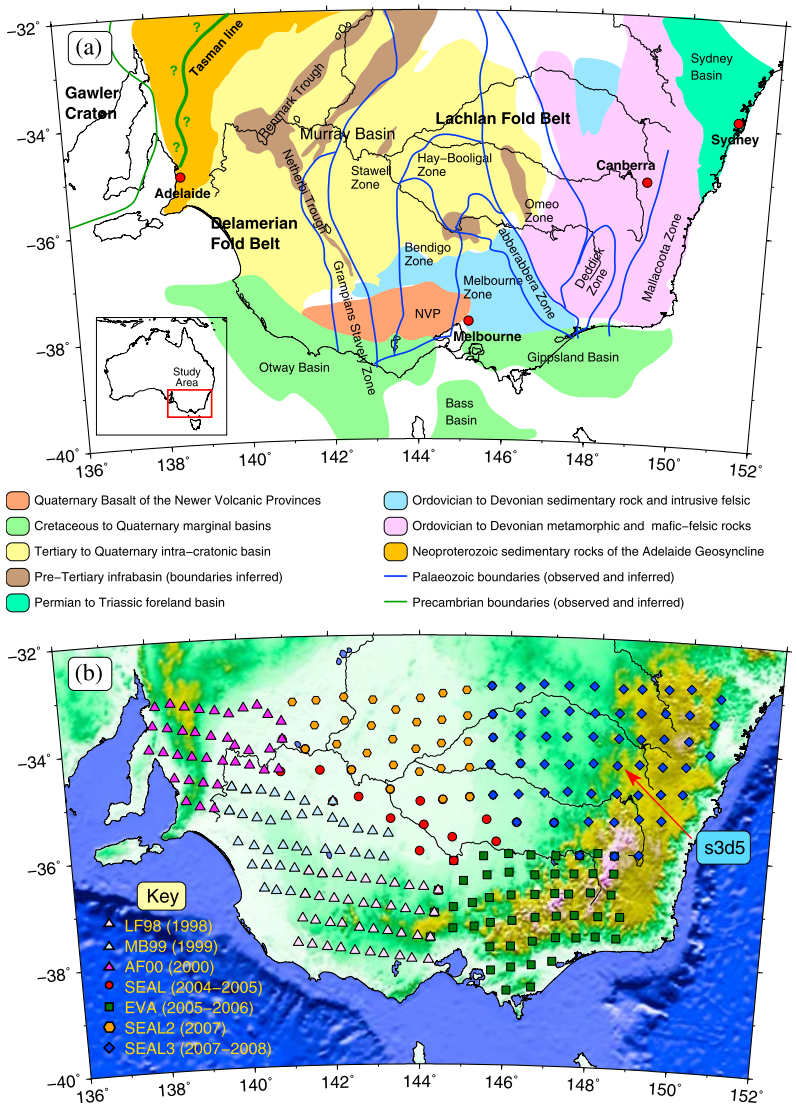

Figure 1. (a) Simplified geological map showing the main rock types, basins and tectonic units present in southeast Australia. Figure 1a is based on maps given by *Knight et al.* [1995], *Foster and Gray* [2000] and *Cayley et al.* [2002]. (b) Location of all WOMBAT stations used in this study. The seven mainland arrays were deployed over a 10 year period, from 1998–2008.

and the average station spacing is 50 km, resulting in the most dense dataset of its kind in the Australian region. The presence of tie stations common to adjacent arrays helps mitigate the variable path coverage, which is dense within each array but less dense near array boundaries, that arises from the sequential nature of the deployments.

[7] The data processing scheme described by *Bensen et al.* [2007] has become the standard approach for ambient noise tomography [e.g., *Villaseñor et al.*, 2007; *Nunziata et al.*, 2009]. In this work, we follow the modus operandi described by these authors with a few slight modifications developed further below. We compute the ambient noise cross-correlation on the vertical component for all simultaneously recording station pairs. The so-called symmetric component is then calculated by averaging the causal and acausal parts of the cross-correlograms [*Bensen et al.*, 2007]. Following *Saygin And Kennett* [2009], we do not apply any normalization prior to the correlation process in order not to alter the spectral content of the data. The extracted waveforms exhibit a dispersed wavetrain which can be interpreted as the Rayleigh wave component of the Green's function (Figure 2a) and may thus be processed by means of conventional surface wave analysis tools.

[8] Group velocities of the Rayleigh wave fundamental mode for periods ranging from 1 to 28 s are extracted (see Figures 2b and 2c) using an automated implementation of the multiple filter technique of *Dziewonski et al.* [1969]. Both the noise correlation function and its time derivative are used to obtain quasi-independent measurements of the group velocities [see *Sabra et al.*, 2005; *Nunziata et al.*, 2009], under the assumption that the phase shift produced by the differentiation does not significantly affect the group velocity signal. The average of the two values for each period and station pair is used as the final group velocity provided that the two measurements do not differ by more than 3%. The complete procedure is implemented in a two-

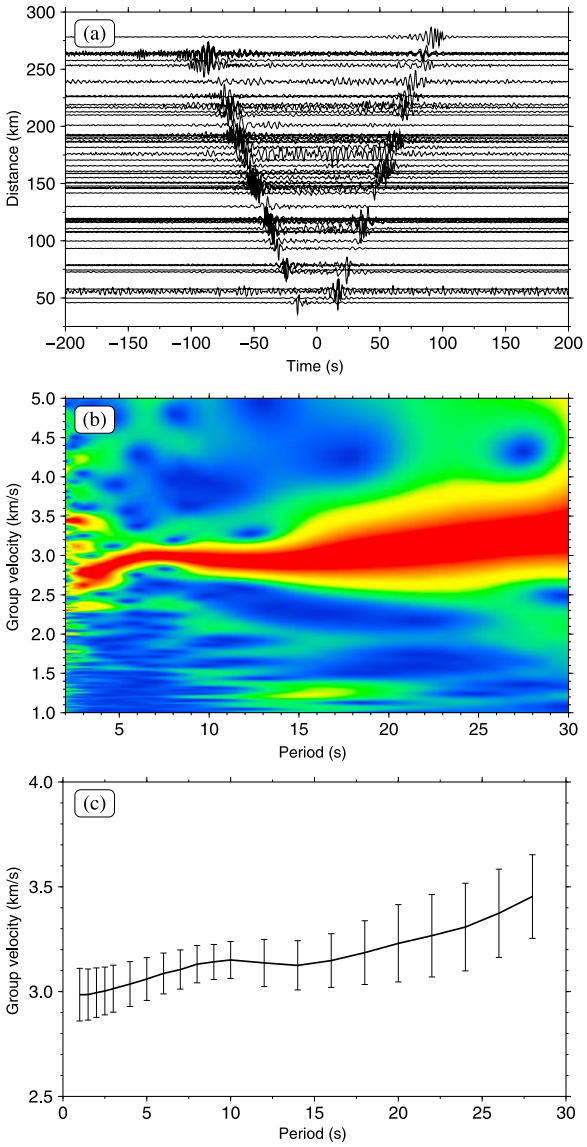

Figure 2. (a) Record sections showing raw cross-correlations between station s3d5 and all other stations of the SEAL3 network (see Figure 1b). The causal and acausal arrivals of the Rayleigh wave are clearly visible in most cases. (b) Frequency-time diagram for two stations in the SEAL array that are separated by 495 km. (c) Average group velocity measurements across all the arrays, with error bars showing one standard deviation of the spread of velocities at various periods.

stage approach; in the first stage, preliminary dispersion curves are constructed and averaged in order to build a phase-matched filter [see *Levshin and Ritzwoller* 2001] which is subsequently applied to the seismograms prior to a second round of traveltime picking. This allows additional dispersion measurements to be included that were discarded during the first stage due to low signal-to-noise ratio.

[9] Group traveltimes are mapped as variations in Rayleigh wave group velocity for different periods using the iterative non-linear tomography scheme described by *Rawlinson et al.* [2008], which accounts for wavefront focusing and defocusing caused by velocity heterogeneity. Smoothly varying cubic B-spline functions are used to describe the velocity continuum, which is controlled by a regular grid of nodes in latitude and longitude.

3. Results and Discussion

[10] Group velocity maps obtained from the WOMBAT ambient noise dataset are shown in Figure 3, for periods 2.5 s, 5s, 10 s and 20 s, along with their associated checkerboard test results. Note that the same absolute colour scale is used for each of the four plots to better facilitate comparison. In general, the images are well resolved at all frequencies, with the exception of the central northern sector of the array, which has the lowest path density. This may be due to the attenuating effects of the Murray Basin sediments which underlie much of the SEAL and SEAL2 arrays (see Figure 1). The gradual decrease in overall resolution with increasing period can be mainly attributed to the need to discard cross-correlations for station pairs that are less than approximately two wavelengths apart.

[11] Figure 3 clearly shows that the average group velocity increases with increasing period, which is in general agreement with Figure 2c. Similar to *Villaseñor et al.* [2007], we interpret the group velocity maps as approximately representing average shear velocities in different depth intervals of the crust. Thus, the 2.5 s image (Figure 3a) represents the top few km of the crust; the 5 s image (Figure 3c) represents an average of the upper crust to a depth of 5–10 km; the 10 s image (Figure 3e) represents the top 5–15 km of the crust, while the 20 s image (Figure 3g) reflects the structure in the depth interval 10–30 km.

[12] A comparison of Figures 3a and 3c with Figure 1 shows that there is good agreement between the broad-scale surface geology and variations in group wavespeed; in particular, correlations exist between the sedimentary basins (or exposed sedimentary rock) and lower group wavespeeds, and regions of metamorphic and igneous exposure and higher group wavespeeds. Both the Sydney and Murray basins stand out quite clearly in the 2.5 s image (Figure 3a), although in the latter case, velocities are not as low, most likely due to the Murray Basin sediment layer being relatively thin in most places. The NVP (Figure 1) corresponds to a region of lower group velocity (Figure 3a), which is most likely a consequence of elevated temperatures associated with recent hot-spot volcanism (for an upper crustal temperature map of the region, see *Saygin and Kennett* [2009]).

[13] The terrain dominated by Ordovician to Devonian metamorphic and mafic-felsic rocks (Figure 1), which corresponds to much of the Great Dividing Range, is clearly revealed in both Figures 3a and 3c as a marked velocity high. The westerly transition to the Melbourne Zone sediments is also visible as a significant decrease in group velocity, particularly in Figure 3a. At longer periods (Figures 3e and 3g), obvious correlations with the surface geology decrease, which is to be expected given the stronger sensitivity to structure at greater depths. The most persistent feature in the 10 s and 20 s images is an elongated lower velocity region in the centre of the Murray Basin, which may be caused by sediments in the thickest part of the basin, although this seems unlikely given the depth sensitivity of the longer period waves. There is little evidence for an equivalent feature in the teleseismic tomography [*Rawlinson et al.*,

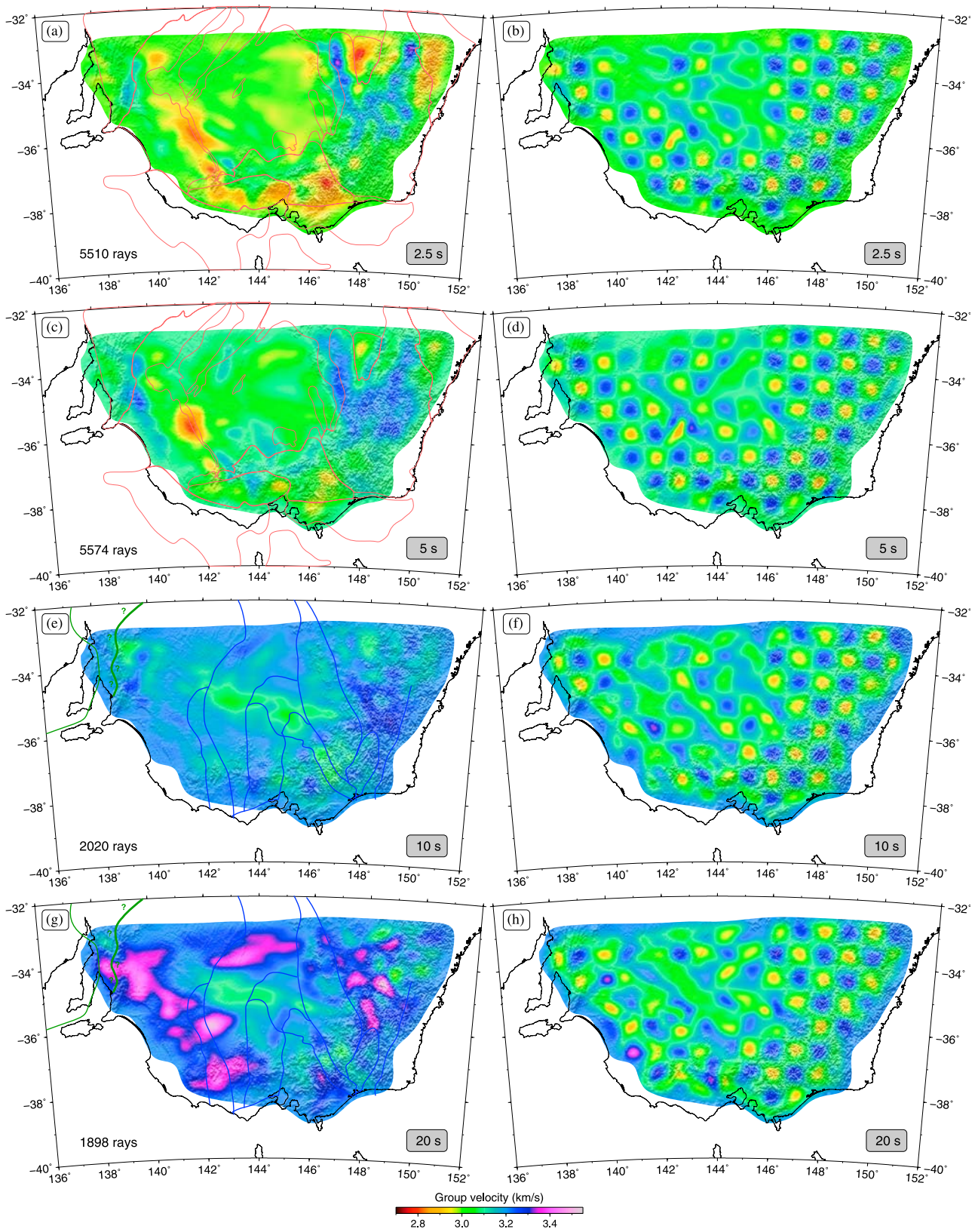

Figure 3. (a, c, e, and g) Group velocity maps and (b, d, f, and h) checkerboard resolution test results for Rayleigh waves ranging in period from 2.5 s to 20 s. All images have been cropped so that velocities outside the combined array region (where there is no path coverage) are not shown. Note that the absolute colour scale used to represent velocity variations is identical for each plot. Boundaries of major surface geological features (taken from Figure 1a) are superimposed on Figures 3a and 3c; similarly, major Palaeozoic boundaries are superimposed on Figures 3e and 3g.

2006a], but this is unsurprising since crustal structure is poorly constrained by arrival time residuals from distant earthquakes.

[14] In the western region of the Murray Basin at mid-upper crustal depths, a marked low velocity anomaly can be observed, which is slightly elongated in the NNW direction in Figure 3a, but more distinct in Figure 3c (centred at about 141.5°E and 35.5°S). This approximately corresponds to the location of the Netherbi Trough, the geometry of which is poorly constrained [*Knight et al.*, 1995]. It is possible that this anomaly is related to part of the infra-basin that is thicker and broader than previously inferred. Earlier work [*Knight et al.*, 1995] has indicated that the Netherbi Trough has hydrocarbon potential, and the low group velocities in the area may be a signature of higher concentrations of organic rich sediments.

[15] The Palaeozoic basement structure in southeast Australia, indicated by the blue lines in Figure 1, has no real presence in the group velocity maps, with the exception of the transition from the Omeo Zone to the Tabberabbera Zone. Each zone contains distinct crustal units [*Foster and Gray*, 2000] that are largely defined by often limited outcrop and potential field data. These crustal units may be distinguished by, for example, different deformational histories, rocks of different ages or type, or differences in structural vergence. The lack of any real signature of zonal boundaries in the group velocity maps at the very least suggests that they are probably not associated with compositional differences at depth. Similarly, the transition between Phanerozoic and Precambrian Australia, which is often represented by the so-called Tasman Line (Figure 1), has no signature in the group velocity maps. However, as Figures 3e and 3g show, the probable location of the transition zone lies near the western edge of the array distribution, so information is limited. Nonetheless, this result is consistent with the continental ambient noise tomography study of *Saygin and Kennett* [2009], and the argument put forward by *Direen and Crawford* [2003] that there is no clearly defined transition between Phanerozoic and Precambrian Australia.

4. Conclusions

[16] We have presented the first ambient noise tomography results from the WOMBAT rolling array experiment in southeast Australia. Using data from a total of 282 stations, high resolution Rayleigh wave group velocity maps have been produced which reveal a variety of structures in the shallow to mid-crust. These include low velocity zones that closely correlate with known sedimentary basins and recent volcanism, and high velocity zones associated with outcropping igneous and metamorphic rocks. Of particular note is the low velocity anomaly associated with the Netherbi Trough, a pre-Tertiary infra-basin concealed beneath the Murray Basin, which has hydrocarbon potential, and the lack of any clear signature of the Palaeozoic building blocks of the continent that have previously been inferred from geological and geophysical analyses of near-surface features. This latter result has important implications for models which attempt to explain the tectonic evolution of the region. Future work will include combining other classes of seismic data extracted from WOMBAT (e.g., teleseismic traveltime residuals, receiver functions) with the ambient noise data in order to jointly constrain crust and upper mantle structure, and the incorporation of new data from on-going deployments in northern New South Wales and Queensland.

References

Bensen, G. D., M. H. Ritzwoller, M. P. Barmin, A. L. Levshin, F. Lin, M. P. Moschetti, N. M. Shapiro, and Y. Yang (2007), Processing seismic ambient noise data to obtain reliable broad-band surface wave dispersion measurements, *Geophys. J. Int.*, *169*, 1239–1260, doi:10.1111/j.1365-246X.2007.03374.x.

Bryan, S. E., A. E. Constantine, C. J. Stephens, A. Ewart, R. W. Schön, and J. Parianos (1997), Early Cretaceous volcano-sedimentary successions along the eastern Australian continental margin: Implications for the break-up of eastern Gondwana, *Earth Planet. Sci. Lett.*, *153*, 85–102.

Cayley, R., D. H. Taylor, A. H. M. VandenBerg, and D. H. Moore (2002), Proterozoic-Early Palaeozoic rocks and the Tyennan Orogeny in central Victoria: The Selwyn Block and its tectonic implications, *Aust. J. Earth Sci.*, *49*, 225–254.

Clifford, P., S. Greenhalgh, G. Houseman, and F. Graeber (2008), 3-D seismic tomography of the Adelaide fold belt, *Geophys. J. Int.*, *172*, 167–186.

Direen, N. G., and A. J. Crawford (2003), The Tasman Line: Where is it, what is it, and is it Australia's Rodinian breakup boundary?, *Aust. J. Earth Sci.*, *50*, 491–502.

Dziewonski, A., S. Bloch, and M. Landisman (1969), A technique for the analysis of transient seismic signals, *Bull. Seismol. Soc. Am.*, *59*(1), 427–444.

Foster, D. A., and D. R. Gray (2000), Evolution and structure of the Lachlan Fold Belt (Orogen) of eastern Australia, *Ann. Rev. Earth Planet. Sci.*, *28*, 47–80.

Glen, R. A. (2005), The Tasmanides of eastern Australia, in *Terrane Processes at the Margins of Gondwana*, edited by A. P. M. Vaughan, P. T. Leat, and R. J. Pankhurst, *Geol. Soc. Spec. Publ.*, *246*, 23–96.

Graeber, F. M., G. A. Houseman, and S. A. Greenhalgh (2002), Regional teleseismic tomography of the western Lachlan Orogen and the Newer Volcanic Province, southeast Australia, *Geophys. J. Int.*, *149*, 249–266.

Kennett, B. L. N., S. Fishwick, A. M. Reading, and N. Rawlinson (2004), Contrasts in mantle structure beneath Australia: Relation to Tasman Lines?, *Aust. J. Earth Sci.*, *51*, 563–569.

Knight, L. A., P. A. McDonald, E. Frankel, and D. H. Moore (1995), A preliminary appraisal of the pre-Tertiary infrabasins beneath the Murray Basin, northwestern Victoria, *VIMP Rep. 16*, Geol. Surv. of Victoria, Victoria, B. C., Canada.

Levshin, A. L., and M. H. Ritzwoller (2001), Automated detection, extraction, and measurement of regional surface waves, *Pure Appl. Geophys.*, *158*, 1531–1545, doi:10.1007/PL00001233.

Nunziata, C., G. D. Nisco, and G. Panza (2009), S-waves profiles from noise cross correlation at small scale, *Eng. Geol.*, *105*(3–4), 161–170, doi:10.1016/j.enggeo.2009.01.005.

Price, R. C., C. M. Gray, and F. A. Frey (1997), Strontium isotopic and trace element heterogeneity in the plains basalts of the Newer Volcanic Province, Victoria, Australia, *Geochim. Cosmochim. Acta*, *61*, 171–192.

Rawlinson, N., and B. L. N. Kennett (2008), Teleseismic tomography of the upper mantle beneath the southern Lachan Orogen, *Australia, Phys. Earth Planet. Inter.*, *167*, 84–97.

Rawlinson, N., and M. Urvoy (2006), Simultaneous inversion of active and passive source datasets for 3-D seismic structure with application to Tasmania, *Geophys. Res. Lett.*, *33*, L24313, doi:10.1029/2006GL028105.

Rawlinson, N., B. L. N. Kennett, and M. Heintz (2006a), Insights into the structure of the upper mantle beneath the Murray Basin from 3D teleseismic tomography, *Aust. J. Earth Sci.*, *53*, 595–604.

Rawlinson, N., A. M. Reading, and B. L. N. Kennett (2006), Lithospheric structure of Tasmania from a novel form of teleseismic tomography, *J. Geophys. Res.*, *111*, B02301, doi:10.1029/2005JB003803.

Rawlinson, N., M. Sambridge, and E. Saygin (2008), A dynamic objective function technique for generating multiple solution models in seismic tomography, *Geophys. J. Int.*, *174*, 295–308.

Sabra, K. G., P. Gerstoft, P. Roux, W. A. Kuperman, and M. C. Fehler (2005), Extracting time-domain Green's function estimates from ambient seismic noise, *Geophys. Res. Lett.*, *32*, L03310, doi:10.1029/2004GL021862.

Saygin, E., and B. Kennett (2009), Ambient seismic noise tomography of Australian continent, *Tectonophysics*, *481*, 116–125, doi:10.1016/j.tecto.2008.11.013.

Shapiro, N. M., M. Campillo, L. Stehly, and M. H. Ritzwoller (2005), High-resolution surface wave tomography from ambient seismic noise, *Science*, *307*, 1615–1618.

Spaggiari, C. V., D. R. Gray, and D. A. Foster (2004), Lachlan Orogen subduction-accretion systematics revisited, *Aust. J. Earth Sci.*, *51*, 549–553.
VandenBerg, A. H. M. (1999), Timing of orogenic events in the Lachlan Orogen, *Aust. J. Earth Sci.*, *46*, 691–701.
Villaseñor, A., Y. Yang, M. H. Ritzwoller, and J. Gallart (2007), Ambient noise surface wave tomography of the Iberian Peninsula: Implications for shallow seismic structure, *Geophys. Res. Lett.*, *34*, L11304, doi:10.1029/2007GL030164.

P. Arroucau, N. Rawlinson, and M. Sambridge, Research School of Earth Sciences, Australian National University, Mills Road, Canberra, ACT 0200, Australia. (nick@rses.anu.edu.au)